Supplement of Atmos. Meas. Tech., 13, 5551–5567, 2020
https://doi.org/10.5194/amt-13-5551-2020-supplement

Atmospheric Measurement Techniques
Open Access
EGU

Supplement of

Nano-hygroscopicity tandem differential mobility analyzer (nano-HTDMA) for investigating hygroscopic properties of sub-10 nm aerosol nanoparticles

Ting Lei et al.

Correspondence to: Yafang Cheng (yafang.cheng@mpic.de), and Juan Hong (juanhong0108@jnu.edu.cn)

Table S1: Deliquescence and efflorescence relative humidity of ammonium sulfate below 100 nm reported by difference studies in temperature ranging from 290-300K

Deliquescence relative humidity (DRH)	Efflorescence relative humidity (ERH)	Technique (initial particle size)	Reference
80-86%* (8 nm) 80-85%* (10 nm) 80-90%* (15 nm) 78-80%* (30 nm) 76-79%* (50 nm)		HTDMA (8.10,15,30,50 nm)	Hämeri et al. (2000) (cf. Figure 2a, 2b, 2c, 2d, and 2e)
76-80%*	65%*	HTDMA (100 nm)	Gysel et al. (2002) (cf. Figure 2)
82% (6 nm) 81% (8 nm) 80% (10 nm) 82% (20 nm) 80% (40 nm) 80% (60 nm)	34% (6 nm) 33% (8 nm) 35% (10 nm) 35% (20 nm) 36% (40 nm) 33% (6 nm)	HTDMA (6,8,10,20,40,60 nm)	Biskos et al. (2006b)
-	27-31%* (43.7 nm) 21-30.7%* (47 nm)	HTDMA (43.7,47 nm)	Gao et al. (2006) (cf. Figure 5)
78-81%*	-	HTDMA (100 nm)	Duplissy et al. (2009) (cf. Figure 4)
77-78%*	-	HTDMA	Duplissy et al. (2009)

		(100 nm)	(cf. Figure 4)
78-80%*	29-34%*	HTDMA (100 nm)	Mikhailov et al. (2009) (cf. Fig4)
77-78%	-	HTDMA (100 nm)	Wu et al. (2011)

-: Not reported

*: Data retrieved from figures in the references

80-86%: Non-prompt deliquescence of 8-nm ammonium sulfate from 80% to 86% RH

27-31%: Non-prompt efflorescence of 43.7-nm ammonium sulfate from 31% to 27% RH

82%: Prompt deliquescence of 6-nm ammonium sulfate at 82% RH

Table S2. Residence time (s) for the water equilibrium for particles with diameter ranging from 6 to 100 nm particles at RH=90% at 25°C

χ	1	0.1	0.01	0.001
100nm	6.26×10^{-6}	3.55×10^{-5}	3.12×10^{-4}	0.00310
60nm	6.04×10^{-6}	3.34×10^{-5}	3.07×10^{-4}	0.00300
20nm	6.03×10^{-7}	5.17×10^{-6}	5.08×10^{-5}	5.07×10^{-4}
10nm	1.88×10^{-7}	1.74×10^{-6}	1.73×10^{-5}	1.72×10^{-4}
8nm	3.10×10^{-8}	1.93×10^{-7}	1.82×10^{-6}	1.81×10^{-5}
6nm	1.48×10^{-8}	1.08×10^{-7}	1.04×10^{-6}	1.03×10^{-5}

Table S3. Average sizing offset between nano-DMAs in the nano-HTDMA system at RH below 10%

	Average sizing offset (nm)[a]	Size agreement between nano-DMA1 and nano-DMA2[b]
100-nm $(NH_4)_2SO_4$	0.619	0.619%
60-nm $(NH_4)_2SO_4$	0.299	0.498%
20-nm $(NH_4)_2SO_4$_	0.278	1.39%
10-nm $(NH_4)_2SO_4$	0.0896	0.897%
8-nm $(NH_4)_2SO_4$	-0.0160	-0.200%
6-nm $(NH_4)_2SO_4$_	0.0840	1.40%

[a] Calculation from $(\overline{D}_{measured\ by\ nano-DMA2} - D_{selected\ by\ nano-DMA1})$

[b] Calculation from $[(\overline{D}_{measured\ by\ nano-DMA2} - D_{selected\ by\ nano-DMA1})/ D_{selected\ by\ nano-DMA1}] \times 100\%$

Table S4. The values of D_m, g_f, and D_m (< 5% RH) of 10-nm ammonium sulfate of Biskos et al. (2006b) system in the different RHs.

Relative humidity	D_m	g_f	D_m (<5 % RH)
25%	10.4	0.991	10.5
76%	10.4	1.02	10.2
78%	10.5	1.03	10.3
80%	13.3	1.29	10.3
44%	11.6	1.12	10.3
35%	11.2	1.08	10.4
34%	10.6	1.01	10.5
32%	10.2	1.00	10.2
31%	10.2	1.00	10.2
30%	10.4	1.00	10.4
29%	10.3	1.00	10.3
24%	10.3	0.997	10.3

Table S5. Uncertainties of nano-DMA voltage (V) and sheath flow rates (Q_{sh}), and calculated size uncertainty.

Size (nm)	Uncertainties in V and Q_{sh}	Uncertainty (Sizing accuracy)
100	2.65×10^3±0.0259 V, 10±0.0200 L min^{-1}	0.200%
60	1.06×10^3±0.0269 V, 10±0.0200 L min^{-1}	0.200%
20	1.31×10^2±0.0152 V, 10±0.0200 L min^{-1}	0.200%
10	3.37×10^1±0.0244 V, 10±0.0200 L min^{-1}	0.213%
8	2.16×10^1±0.0373 V, 10±0.0200 L min^{-1}	0.264%
6	1.22×10^1±0.0692 V, 10±0.0200 L min^{-1}	0.601%

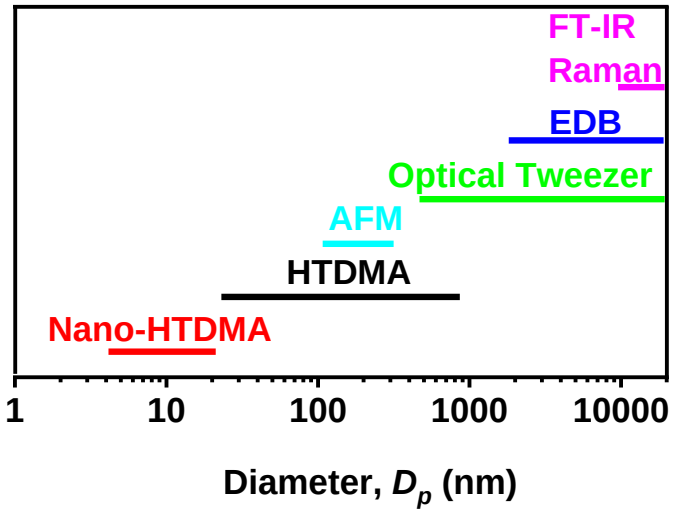

Figure S1. Methods for measuring hygroscopicity of atmospheric aerosol particles in different size (D_p).

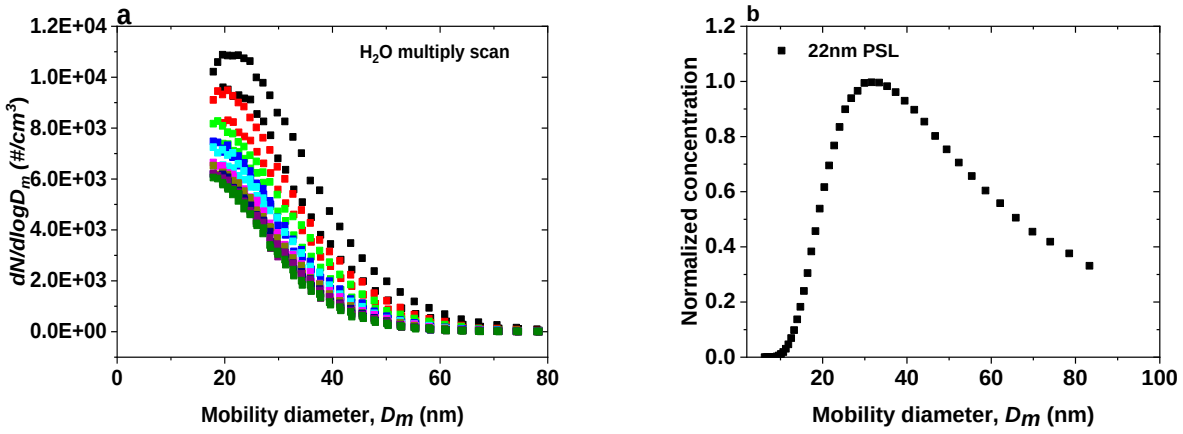

Figure S2. (a) Number concentration scanned for water nanoparticles by the nano-DMA2 at RH below 5 % at 298 K. **(b)** Normalized number size distribution scanned for 22-nm PSL nanoparticles by nano-DMA2 after calibration.

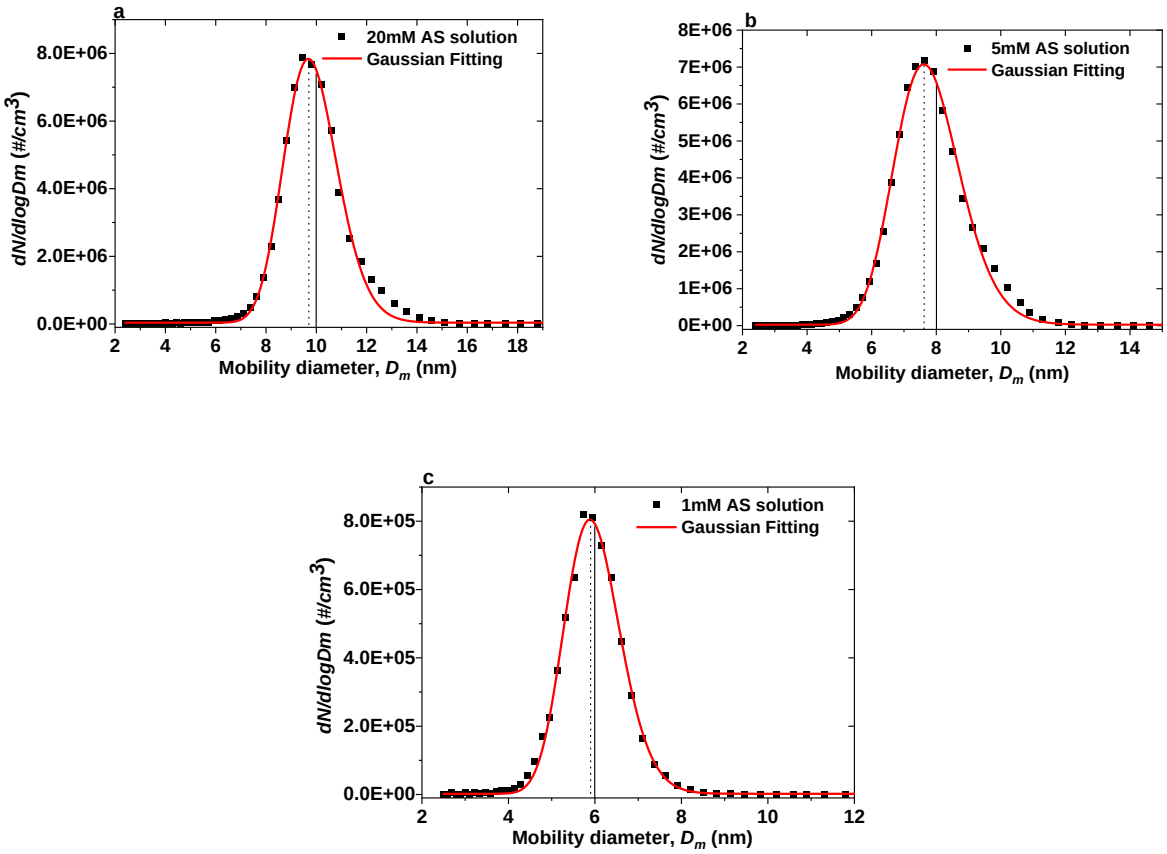

Figure S3. Number size distribution of ammonium sulfate (AS) nanoparticles (black solid square) generated by the electrospray. **(a)** 20mM, **(b)** 5mM, and **(c)** 1mM AS solution. The dotted line marks peak diameter from the Gaussian fits for the scan (red curve). The black solid lines mark the diameters of the monodispersed nanoparticles selected by the nano-DMA1.

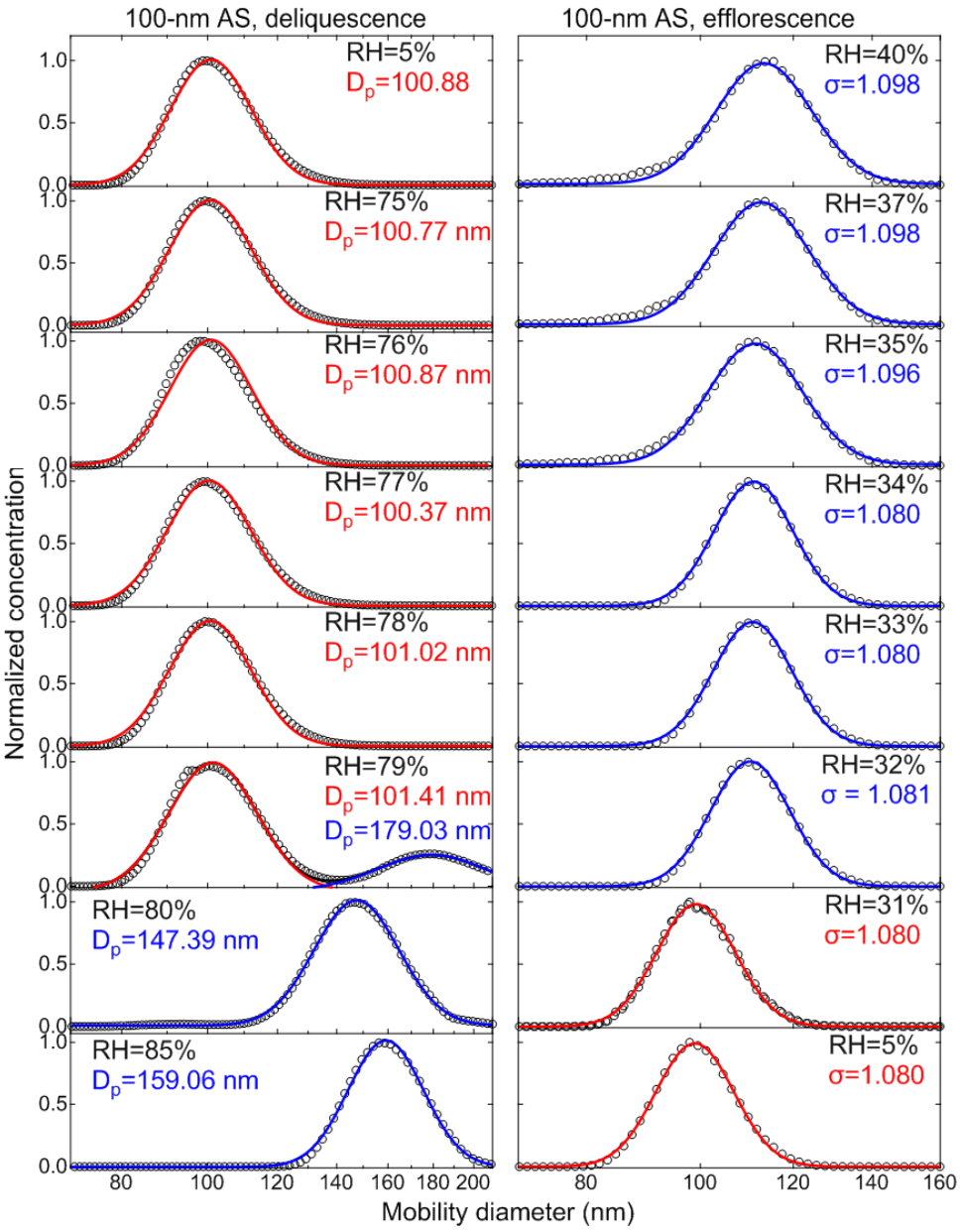

Figure S4. Deliquescence-mode **(a)** and efflorescence-mode **(b)** of 100-nm ammonium sulfate (AS) aerosol nanoparticles. The measured (black square) and fitted (solid lines) normalized size distribution are shown for increasing RH (5%→X%, where X is the RH value given in each panel) and decreasing RH (5%→97%→X%, where X is the RH value given in each panel), respectively. The red and blue lines represent the aerosol nanoparticles in the solid and liquid state, respectively.

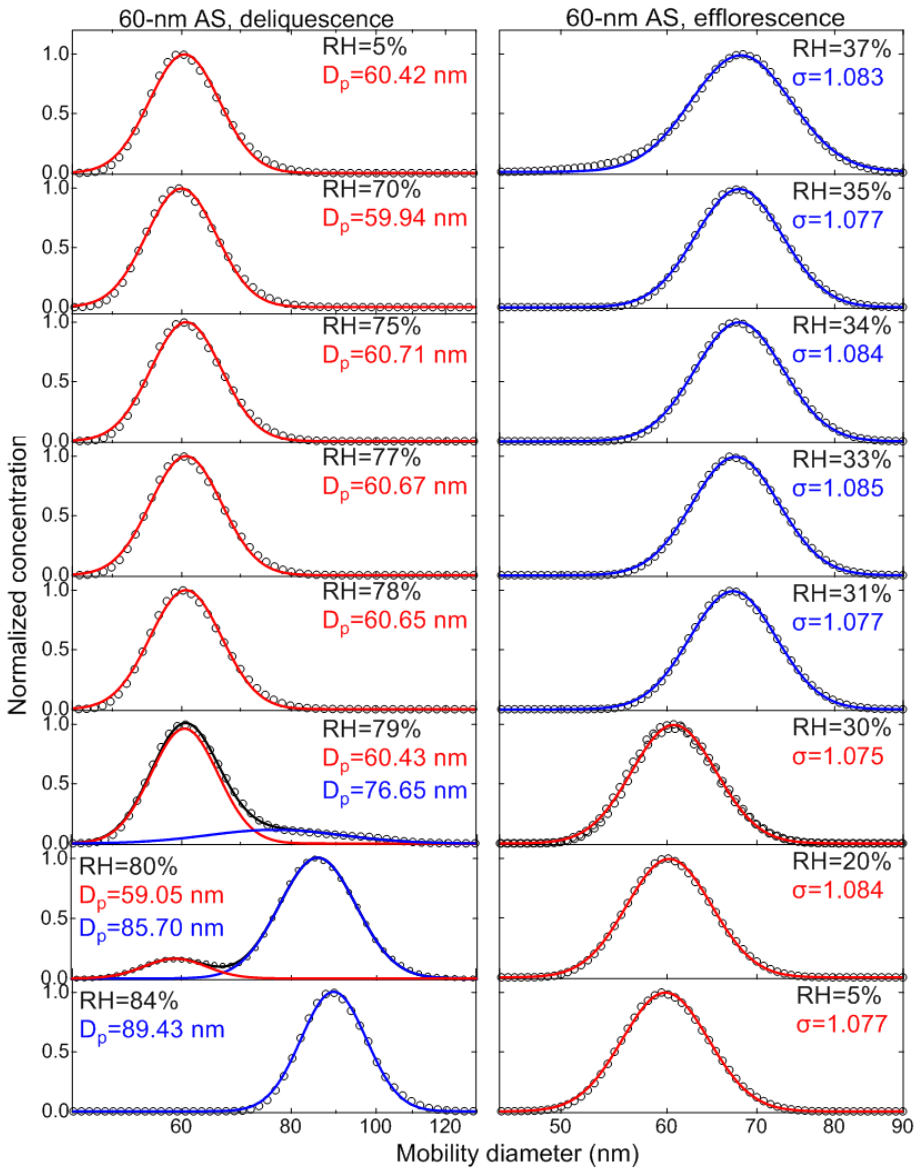

Figure S5. Deliquescence-mode **(a)** and efflorescence-mode **(b)** of 60-nm ammonium sulfate (AS) aerosol nanoparticles. The measured (black square) and fitted (solid lines) normalized size distribution are shown for increasing RH (5%→X%, where X is the RH value given in each panel) and decreasing RH (5%→97%→X%, where X is the RH value given in each panel), respectively. The red and blue lines represent the aerosol nanoparticles in the solid and liquid state, respectively.

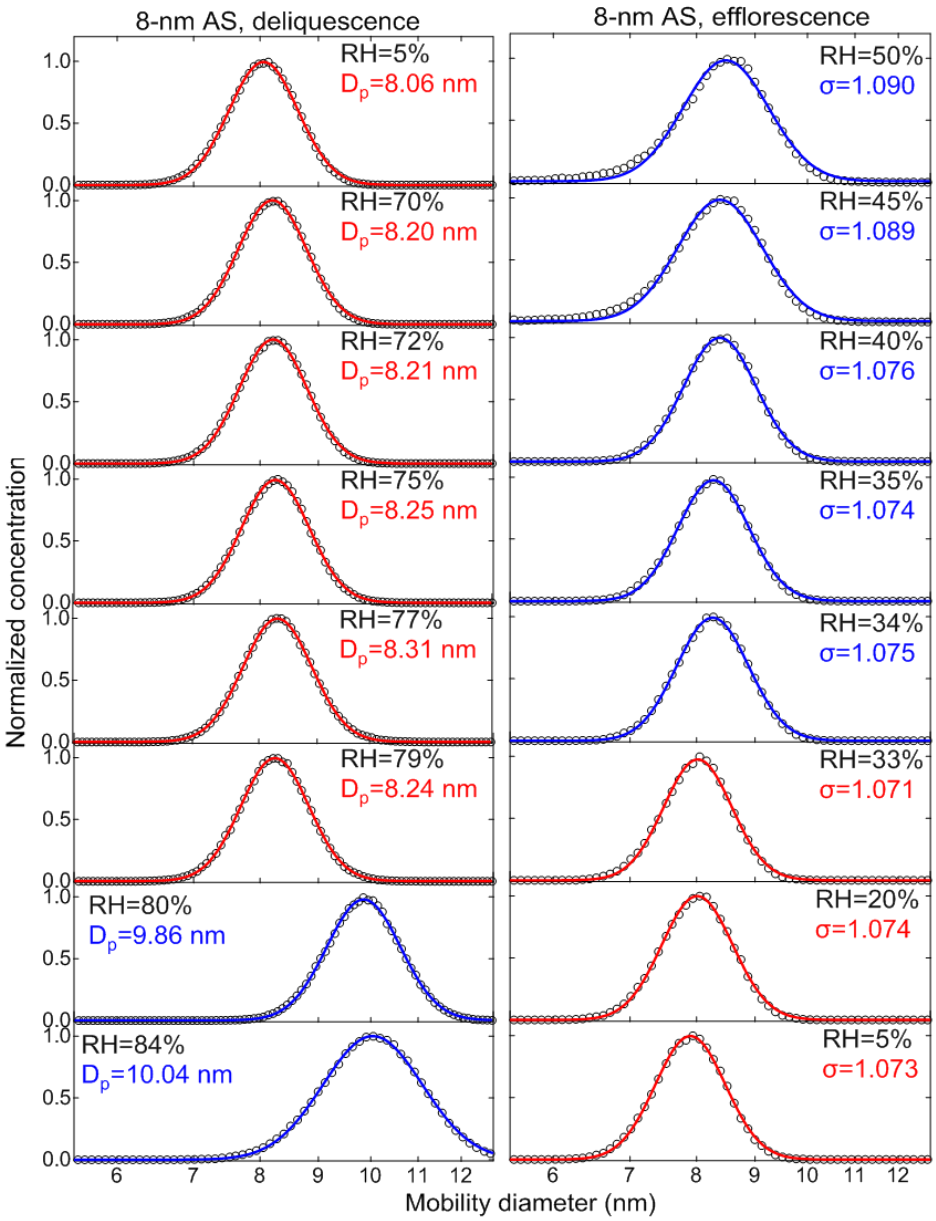

63

64

65 **Figure S6.** Deliquescence-mode **(a)** and efflorescence-mode **(b)** of 8-nm ammonium sulfate (AS) aerosol nanoparticles.
66 The measured (black square) and fitted (solid lines, single-mode log-normal fit) normalized size distribution are shown
67 for increasing RH (5%→X%, where X is the RH value given in each panel) and decreasing RH (5%→97%→X%,
68 where X is the RH value given in each panel), respectively. The red and blue lines represent the aerosol nanoparticles
69 in the solid and liquid state, respectively.

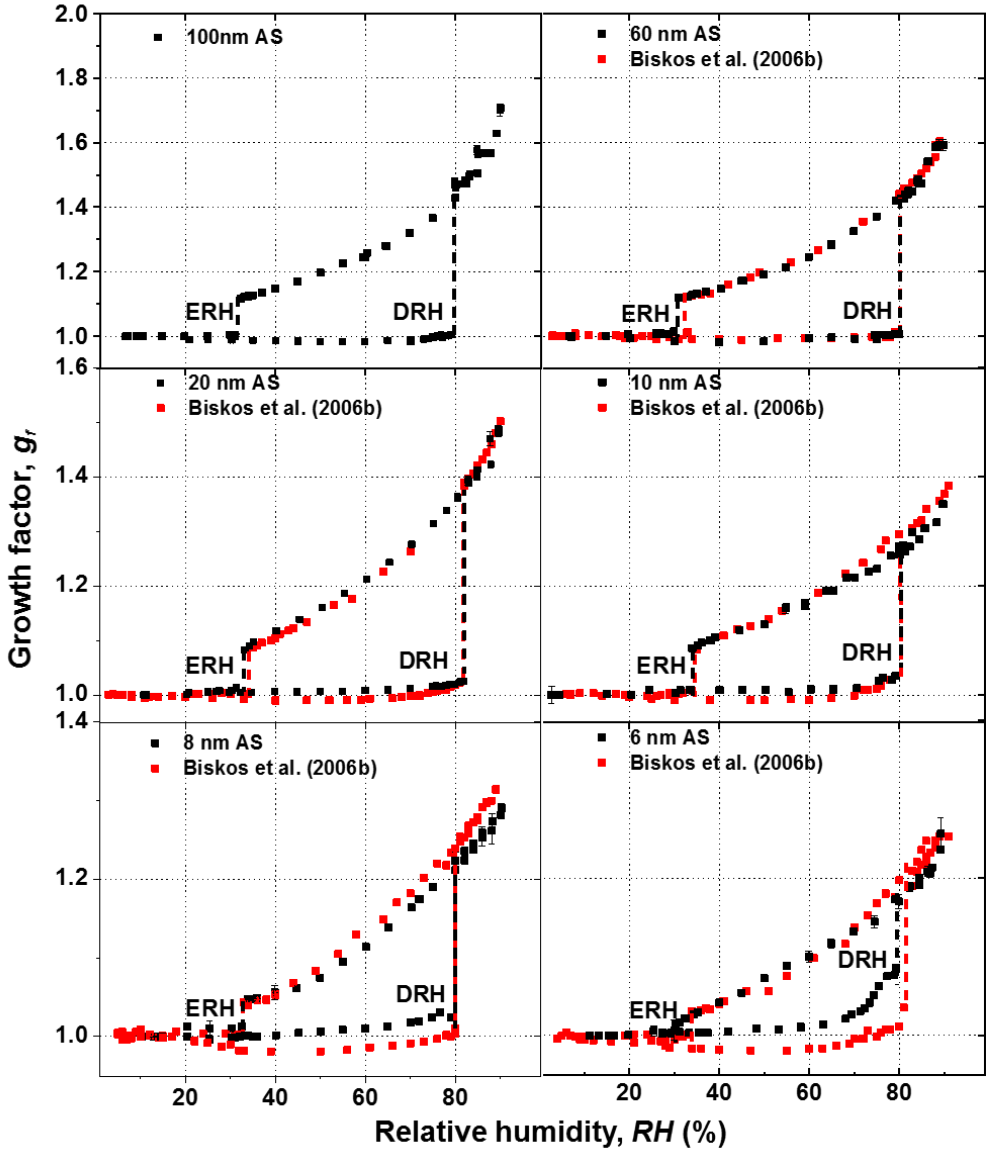

Figure S7. Mobility-diameter hygroscopic growth factors (g_r, black squares), deliquescence and efflorescence relative humidity (DRH&ERH, black dashed lines) of ammonium sulfate (AS) nanoparticles with dry diameter from 6 to 100 nm, respectively. Red squares and dashed lines show the respective results from Biskos et al. (2006b).

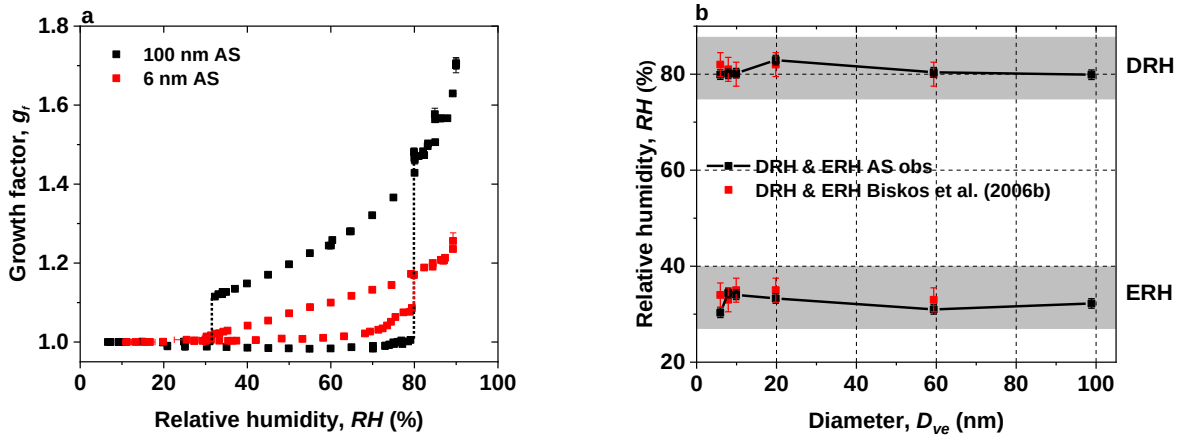

Figure S8. (a) Comparison of mobility-diameter hygroscopic growth factors (g_f) of 100-nm (black square) with 6-nm (red square) ammonium sulfate (AS) nanoparticles. **(b)** Dependence of deliquescence and efflorescence relative humidity (DRH&ERH) of ammonium sulfate (AS) on dry volume equivalent diameter (D_{ve}). The measured DRH and ERH of ammonium sulfate within RH uncertainty (black line + black square) compared with data from Biskos et al. (2006b) (red square) in the volume equivalent diameter with shape factor (χ=1.02) range from 5 to 100 nm.

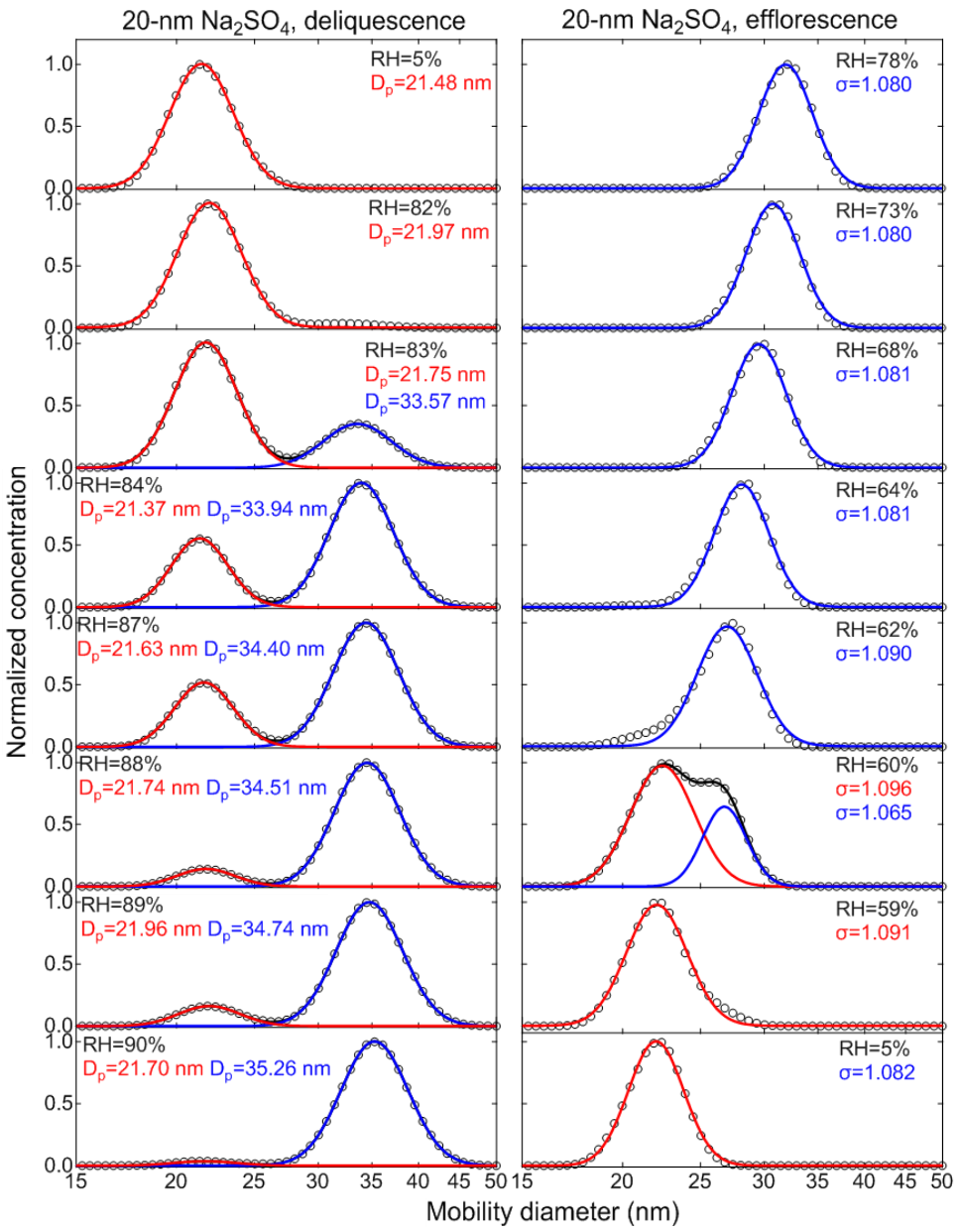

Figure S9. Deliquescence-mode **(a)** and efflorescence-mode **(b)** of 20-nm sodium sulfate aerosol nanoparticles. The measured (black square) and fitted (solid lines) normalized size distribution are shown for increasing RH (5%→X%, where X is the RH value given in each panel) and decreasing RH (5%→97%→X%, where X is the RH value given in each panel), respectively. Red/blue solid line is fitted by a single-mode log-normal fit. Red, blue, and black lines are fitted by a double-mode log-normal fit. The red and blue lines represent the aerosol nanoparticles in the solid and liquid state, respectively. The voltage applied to the nano-DMAs (0-12500 V) is kept within ±1% around the set value shown in the voltage meter.

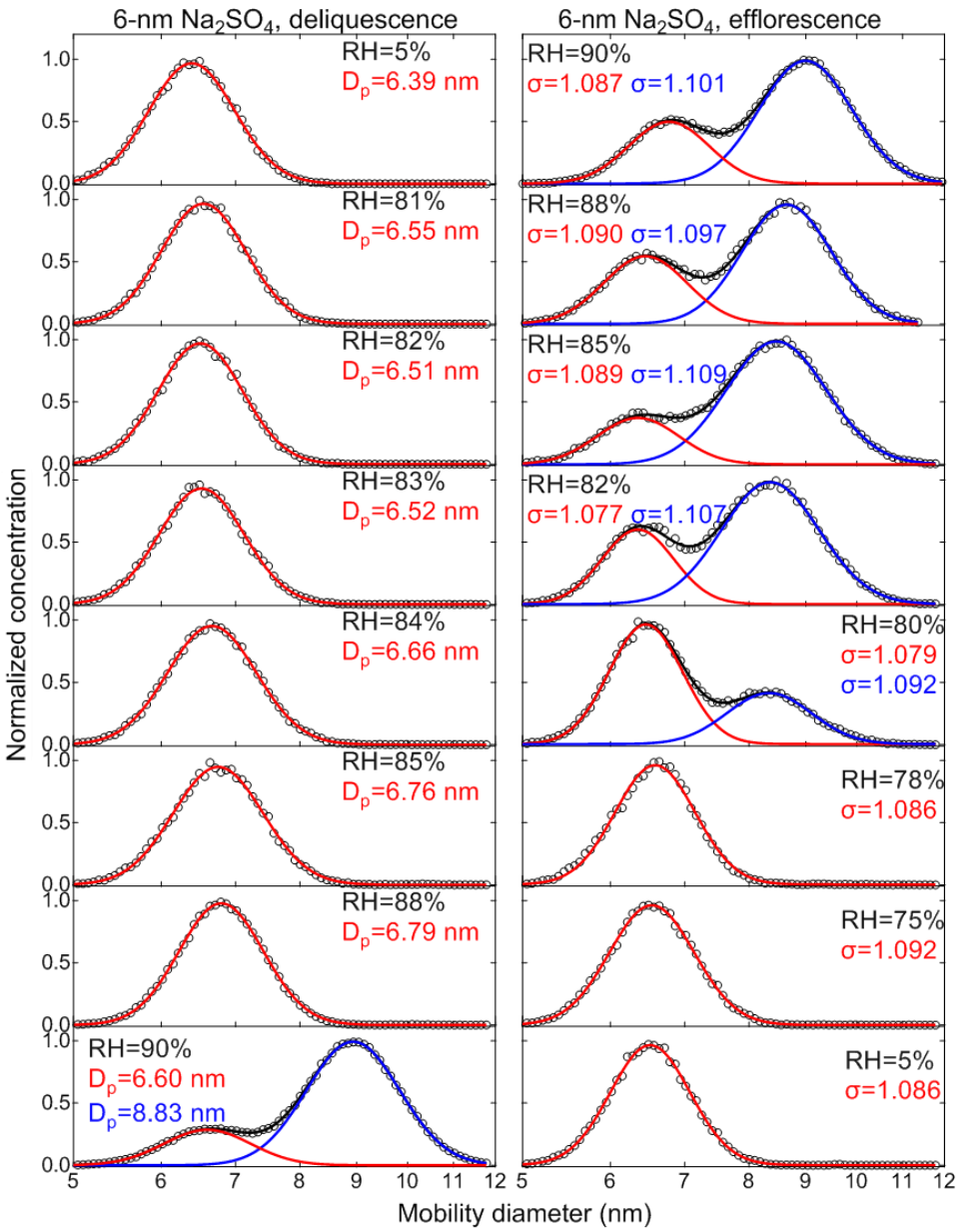

Figure S10. Deliquescence-mode **(a)** and efflorescence-mode **(b)** of 6-nm sodium sulfate aerosol nanoparticles. The measured (black square) and fitted (solid lines) normalized size distribution are shown for increasing RH (5%→X%, where X is the RH value given in each panel) and decreasing RH (5%→97%→X%, where X is the RH value given in each panel), respectively. Red/blue solid line is fitted by a single-mode log-normal fit. Red, blue, and black lines are fitted by a double-mode log-normal fit. The red and blue lines represent the aerosol nanoparticles in the solid and liquid state, respectively. The voltage applied to the nano-DMAs (0-350 V) is kept within ±1% around the set value shown in the voltage meter.

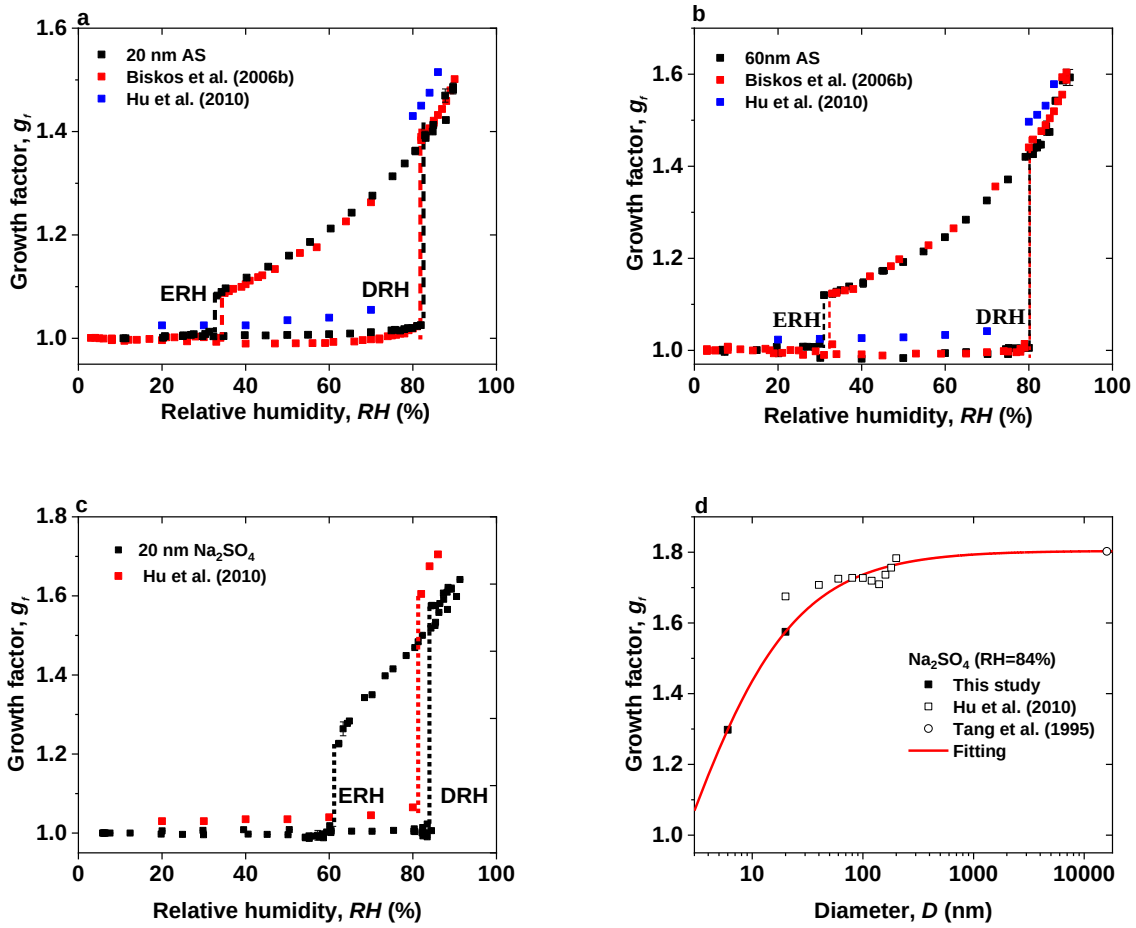

Figure S11. (a) Comparison of mobility-diameter hygroscopic growth factors (g_f) of 20-nm **(a)** and 60-nm **(b)** ammonium sulfate (AS) nanoparticles with Biskos et al. (2006b) and Hu et al. (2010). (black squares: in this study; red square: Biskos et al. (2006b); blue square: Hu et al. (2010)). **(c)** Comparison of mobility-diameter hygroscopic growth factors of 20-nm Na_2SO_4 nanoparticles with Hu et al. (2010). (black squares: in this study; red square: Hu et al. (2010)). **(d)** Mobility-diameter hygroscopic growth factors of Na_2SO_4 nanoparticles with diameter from 6 nm to 14~16 um at 84% RH (black solid squares: in this study; black open square: Hu et al. (2010); black open cycle: Tang et al. (1995)). A fitting equation ($g_f = \frac{1.804}{1+(0.5267*D)^{-0.8194}}$) based on this study at 6-nm, 20-nm Na_2SO_4, and 14~16 um data from Tang et al. (1995).

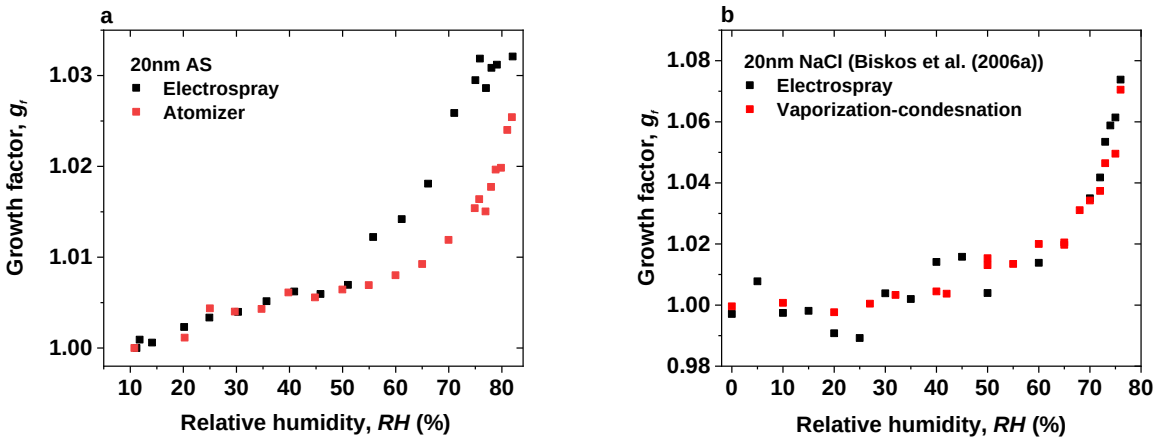

Figure S12. Hygroscopic growth factors of 20-nm **(a)** ammonium sulfate (AS) nanoparticles from our study and **(b)** sodium chloride (NaCl) nanoparticles from Biskos et al. (2006a) using the different generation methods prior to deliquescence of ammonium sulfate.

S1. Calculation of average sizing offset of 10-nm AS

The mobility growth factor (g_f) is given by:

$$g_f = \frac{D_m(RH)}{D_m(<10\ \%\ RH)} \quad \text{(S1)}$$

g_f was from the data of Biskos et al. (2006b) in the different RHs (see the SI. Fig.5). D_m was retrieved the data of Biskos et al. (2006b) in the different RHs (see the SI. Fig.2) as follows:

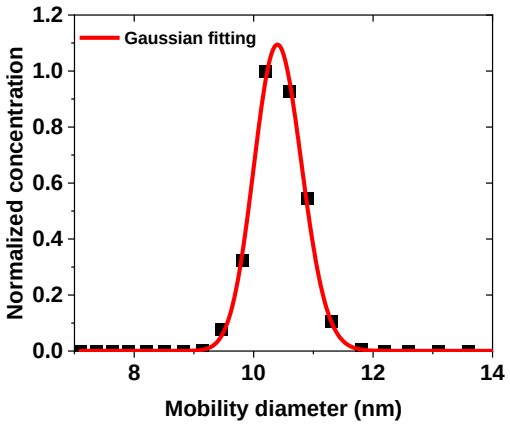

Figure S13. Measured (black square) and fitted (red solid line) normalized number size distributions are show for ammonium sulfate aerosol particles at 25% RH. The black square symbols show the data of Biskos et al. (2006b) (see the S1. Fig. 2).

Therefore, the initial dry mobility diameter (D_m (< 5% RH)) was obtained using Eq. (S1) based on values of g_f and D_m in the different RHs (see SI. S1. Table S4). We further calculated the average sizing offset of 10-nm ammonium sulfate of Biskos et al. (2006b) system based on the values of D_m (< 5% RH). The average sizing offset of 10-nm was ~3.25%.

S2. Calculation of sizing accuracy of sub-100 nanoparticles

Knutson and Whitby (1975) proposed the following theoretical differential mobility analyzer (DMA) transfer function and showed that sizing is crucially depend on sheath flow rates and high voltage (HV) applied to the DMA.

$$z_p^* = \frac{Q_{sh} ln\frac{r_2}{r_1}}{2\pi LV} \quad \text{(S2)}$$

$$z_p^* = \frac{neC_c}{3\pi\mu d_p^*} \quad \text{(S3)}$$

$$d_p^* = \frac{2VLnec_c}{3\mu Q_{sh} ln\frac{r_2}{r_1}} \quad \text{(S4)}$$

where z_p^* is the central electrical mobility, Q_{sh} is the sheath flow rate, V is the applied voltage, L is the length of the classification region within the DMA, and r_1 and r_2 are the inner and outer radii of the DMA annulus, respectively. n is the number of elementary charges of particles. e is the elementary charges. C_c is the slip correction. μ is the flow viscosity. d_p^* is the mean particle mobility diameter.

According to Eq. (S4) above, we use the following error propagation formula ((Taylor and Taylor, 1997) to calculate the uncertainties in sizing of nanoparticles. In our study, the flow accuracy of mass flow meter (TSI series 4000) is within ±2%. The deviation of voltage applied to the nano-DMAs (0-12500 V, 0-350 V) varies around the set value when test with voltage power supply (HCE 0-12500, HCE 0-350, Fug Electronic) shown in Table S5. Thence, the uncertainties in sizing of nanoparticles are obtained based on the following Eq. (S5) as shown in Table S5.

$$\frac{\delta d}{d} = \sqrt{\left(\frac{\delta V}{V}\right)^2 + \left(\frac{\delta Q_{sh}}{Q_{sh}}\right)^2} \quad \text{(S5)}$$

Reference:

Biskos, G., Paulsen, D., Russell, L. M., Buseck, P. R., and Martin, S. T.: Prompt deliquescence and efflorescence of aerosol nanoparticles, Atmos. Chem. Phys., 6, 4633–4642, https://doi.org/10.5194/acp-6-4633-2006, 2006b.

Duplissy, J., Gysel, M., Sjogren, S., Meyer, N., Good, N., Kammermann, L., Michaud, V., Weigel, R., Martins dos Santos, S., Gruening, C., Villani, P., Laj, P., Sellegri, K., Metzger, A., McFiggans, G. B., Wehrle, G., Richter, R., Dommen, J., Ristovski, Z., Baltensperger, U., and Weingartner, E.: Intercomparison study of six HTDMAs: results and recommendations, Atmos. Meas. Tech., 2, 363–378, https://doi.org/10.5194/amt-2-363-2009, 2009.

Gao, Y. G, Chen, S. B., and Yu, L. E.: Efflorescence relative humidity for ammonium sulfate particles, J. Phys. Chem. A, 110, 7602– 7608, https://doi.org/10.1021/jp057574g, 2006.

Gysel, M., Weingartner, E., and Baltensperger, U.: Hygroscopicity of aerosol particles at low temperatures. 2. Theoretical and experimental hygroscopic properties of laboratory generated aerosols, Environ. Sci. Technol., 36, 63–68, doi:10.1021/es010055g, 2002.

Hämeri, K., Väkevä, M., Hansson, H.-C., and Laaksonen, A.: Hygroscopic growth of ultrafine ammonium sulfate aerosol measured using an ultrafine tandem differential mobility analyzer, J. Geophys. Res., 105, 22 231–22 242, 2000.

Hu, D. W., Qiao, L. P., Chen, J.-M., Ye, X. N, Yang, X., Cheng, T. T., and Fang, W.: Hygroscopicity of inorganic aerosols: size and relative humidity effects on the growth factor, Aerosol Air Qual. Res., 10, 255−264. 2010.

Knutson, E. O. and Whitby, K. T.: Aerosol classification by electric mobility: apparatus, theory, and applications, J. Aerosol Sci., 6, 443–451, 1975.

Mikhailov, E., Vlasenko, S., Martin, S. T., Koop, T., and Pöschl, U.: Amorphous and crystalline aerosol particles interacting with water vapor: conceptual framework and experimental evidence for restructuring, phase transitions and kinetic limitations, Atmos. Chem. Phys., 9, 9491–9522, https://doi.org/10.5194/acp-9-9491-2009, 2009.

Tang, I. N., Fung, K. H., Imre, D. G., and Munkelwitz, H. R.: Phase transformation and metastability of hygroscopic microparticles, Aerosol Sci. Technol., 23, 443–453, 1995.

Taylor, J. R. and Taylor, S. L. L. J. R.: Introduction To Error Analysis: The Study of Uncertainties in Physical Measurements, University Science Books, 1997.

Wu, Z. J., Nowak, A., Poulain, L., Herrmann, H., and Wiedensohler, A.: Hygroscopic behavior of atmospherically relevant water-soluble carboxylic salts and their influence on the water uptake of ammonium sulfate, Atmos. Chem. Phys., 11, 12617– 12626, https://doi.org/10.5194/acp-11-12617-2011, 2011.